Simulating algal dynamics within a Bayesian framework to evaluate controls on estuary productivity

Alexey Katin[a], Dario Del Giudice[a], Nathan S. Hall[b], Hans W. Paerl[b], Daniel R. Obenour[a]

[a]Department of Civil, Construction, & Environmental Engineering, North Carolina State University, Raleigh, NC 27695, USA.

[b]University of North Carolina at Chapel Hill, Institute of Marine Sciences, 3431 Arendell St., Morehead City, NC 28557, USA

Corresponding author: Alexey Katin (akatin@ncsu.edu)

Katin, A., Del Giudice, D., Hall, N. S., Paerl, H. W., & Obenour, D. R. (2021). Simulating algal dynamics within a Bayesian framework to evaluate controls on estuary productivity. Ecological Modelling, 447, 109497. https://doi.org/10.1016/j.ecolmodel.2021.109497

Abstract

The Neuse River Estuary (North Carolina, USA) is a valuable ecosystem that has been affected by the expansion of agricultural and urban watershed activities over the last several decades. Eutrophication, as a consequence of enhanced anthropogenic nutrient loadings, has promoted high phytoplankton biomass, hypoxia, and fish kills. This study compares and contrasts three models to better understand how nutrient loading and other environmental factors control phytoplankton biomass, as chl-*a*, over time. The first model is purely statistical, while the second model mechanistically simulates both chl-*a* and nitrogen dynamics, and the third additionally simulates phosphorus. The models are calibrated to a multi-decadal dataset (1997-2018) within a Bayesian framework, which systematically incorporates prior information and accounts for uncertainties. All three models explain over one third of log-transformed chl-*a* variability, with the mechanistic models additionally explaining the majority of the variability in bioavailable nutrients ($R^2 > 0.5$). By disentangling the influences of riverine nutrient concentrations, flows, and loadings on estuary productivity we find that concentration reductions, rather than total loading reductions, are the key to controlling estuary chl-*a* levels. The third model indicates that the estuary, even in its upstream portion, is rarely phosphorus limited, and will continue to be mostly nitrogen limited even under a 30% phosphorus reduction scenario. This model also predicts that a 10% change in nitrogen loading (flow held constant) will produce an approximate 4.3% change in estuary chl-*a* concentration, while the statistical model suggests a larger (10%) effect. Overall, by including a more detailed representation of environmental factors controlling algal growth, the mechanistic models generate chl-*a* forecasts with less uncertainty across a range of nutrient loading scenarios. Methodologically, this study advances the use of Bayesian methods for modeling daily eutrophication dynamics of an estuarine system over a multi-decadal period.

Keywords

eutrophication, phytoplankton, modeling, Bayesian inference, nutrient management, Neuse River Estuary

1 Introduction

Estuarine systems are productive environments that are vital to coastal communities, serving as habitats for wildlife, supporting commercial fisheries, and providing recreational opportunities. However, these systems can be degraded by eutrophication, which is defined as an increase in the supply of organic matter to an ecosystem (Nixon, 1995). Eutrophication is influenced by a combination of factors, including shifts in hydrologic regime that affect transport of nutrients and organic matter, and increases in nutrient loadings resulting from over-fertilization of crops and human and livestock waste (Bricker et al., 1999; de Jonge et al., 2002; Rabalais et al., 2009). Consequently, elevated levels of nutrients in coastal and estuarine waters enhance phytoplankton production, often resulting in harmful algal blooms (Heisler et al., 2008; Paerl et al., 2018b) and expansion of hypoxic "dead" zones (Rabalais et al., 2010).

The Neuse River Estuary (NRE), located in eastern North Carolina (NC), USA, has experienced severe problems including algal blooms, hypoxia, and consequently finfish and shellfish kills (Borsuk et al., 2003; Eby and Crowder, 2002; Lung and Paerl, 1988; Paerl et al., 1995; Selberg et al., 2001). Excessive nutrient loadings are considered the main cause of these water quality issues (Paerl et al., 1998; Rudek et al., 1991). While riverine total phosphorus (TP) concentrations substantially decreased following management actions in the 1980s, nitrogen loadings increased (Borsuk et al., 2001). Beginning in the mid-1990s, extensive monitoring and modeling was conducted to support development of a Total Maximum Daily Load (TMDL),

ultimately requiring a 30% reduction in total nitrogen (TN) delivered to the NRE (NCDWQ, 2001). A decade after TMDL completion, point sources of nitrogen have decreased, but agricultural non-point sources remain problematic (Strickling and Obenour, 2018) and organic nitrogen concentrations have increased (Lebo et al., 2012). As a result, chlorophyll *a* (chl-*a*) concentrations exceed the State criterion of 40 μg/L for more than the allowed 10% of collected samples (Deamer, 2009), and hypoxia and fish kills remain common in the estuary (Katin et al., 2019; Paerl et al., 2018a; Rachels and Ricks, 2018).

The modeling studies developed for the TMDL possessed some limitations, which made them suboptimal for predicting system responses under changing conditions (Stow et al., 2003). The mechanistic models lacked comprehensive uncertainty quantification (Bowen and Hieronymus, 2003; Wool et al., 2003), while a more empirical model did not explicitly represent several biophysical processes (Borsuk et al., 2003). At the same time, we note that one of these studies indicated that the 30% loading reduction suggested by the TMDL would not achieve compliance with the NC chl-*a* criterion (Borsuk et al., 2003, 2002). Additionally, while existing research recognizes the critical role of riverine discharge in controlling chl-*a*, affecting both residence times and nutrient delivery in the NRE, multiple studies showed a weak empirical relationship between riverine nutrients and chl-*a* concentration (Borsuk et al., 2004; Peierls et al., 2012). Given these considerations, new modeling approaches leveraging multiple decades of monitoring data are needed to refine our understanding of how the system will respond to changes in nutrient loading.

The Bayesian modeling framework is recognized as an important tool for improving our capacity to predict and manage eutrophication in aquatic systems (Arhonditsis et al., 2008; Parslow et al., 2013). It allows for updating prior knowledge about model parameters given available data

and obtaining probabilistic predictions (Gelman et al., 2013; Kruschke, 2015). Recent enhancements in computing power have made it possible to calibrate increasingly complex mechanistic models within a Bayesian framework (Malve et al., 2007; Ramin et al., 2011). However, recent Bayesian phytoplankton modeling efforts usually have limited spatio-temporal scope and resolution. Spatially, systems are typically represented as a single mixed reactor, e.g. lake or bay, without accounting for longitudinal variability (Arhonditsis et al., 2007; Del Giudice et al., 2021; Fiechter et al., 2013). Temporally, such models are normally calibrated to a small number of years (Yang et al., 2016), and/or use relatively large (e.g., monthly) time steps (Li et al., 2015).

In this study, we develop a process-based eutrophication model that simulates chl-*a* and nutrient dynamics at a daily time scale over multiple decades. We compare and contrast this process-based model with a statistical piecewise regression model inspired by previous studies of the estuary (Borsuk et al., 2004; Peierls et al., 2012). Both types of models are calibrated to an extensive multi-decadal dataset within a Bayesian framework and produce probabilistic parameter estimates and predictions. These models are used to enhance our understanding of system dynamics. Specifically, we: (1) assess the relative importance of riverine flow, nutrient loading, and concentration in determining estuary production along a longitudinal gradient, (2) quantitatively evaluate the roles of nitrogen, phosphorus, light, and temperature in controlling seasonal patterns in algal abundance, and (3) assess the changes in phytoplankton biomass and probability of meeting NC chl-*a* criteria under various nutrient loading reduction scenarios.

2 Methods

We developed three eutrophication models to predict algal dynamics for the study site. Model 1 is a purely statistical model (Bayesian piecewise regression) and Models 2 and 3 are mechanistic (process-based) models with varying nutrient considerations. In the following subsections, data sources and model segmentations are first specified, including boundary conditions for Models 2 and 3. Then, the deterministic form of each model is specified along with the Bayesian parameter estimation procedure, which is implemented in R (R Core Team, 2019). Finally, model performance assessment and loading scenarios are described.

2.1 Data and estuary segmentation

Model inputs and boundary conditions were estimated using data obtained from several programs and institutions. Measurements of nutrients, chl-*a*, salinity, temperature, and light extinction spanning almost 22 years (January 1, 1997 – September 29, 2018) were collected approximately biweekly (twice per month) along the NRE by the Modeling and Monitoring Program (ModMon, 2019). Neuse River discharge data for the period of interest were retrieved from United States Geographical Survey station 02091814 at Fort Barnwell (USGS, 2019), which is located 35 km upstream of the study area, while meteorological data were obtained from a weather station (KNKT) through the North Carolina Climate Office (NCCO, 2019) (Fig. 1). Discharge (i.e., flow) was corrected by using the ratio of the total estuary watershed to the Fort Barnwell watershed (1.18) to account for ungauged flow (Bales and Robbins, 1999). Daily riverine nitrogen, phosphorus, and chl-*a* concentrations were estimated using WRTDS (Hirsch and De Cicco, 2015) based on water quality data from ModMon station “0”, located 12 km upstream of the upper model boundary. Daily water temperatures were estimated based on regressions with air

temperature, as in Katin et al. (Katin et al., 2019). The NRE was segmented longitudinally (Fig. 1, Table S1), similar to previous studies (Borsuk et al., 2002; Stow et al., 2003). For each sampling date, segment concentrations were determined by averaging the values from the two stations in each segment.

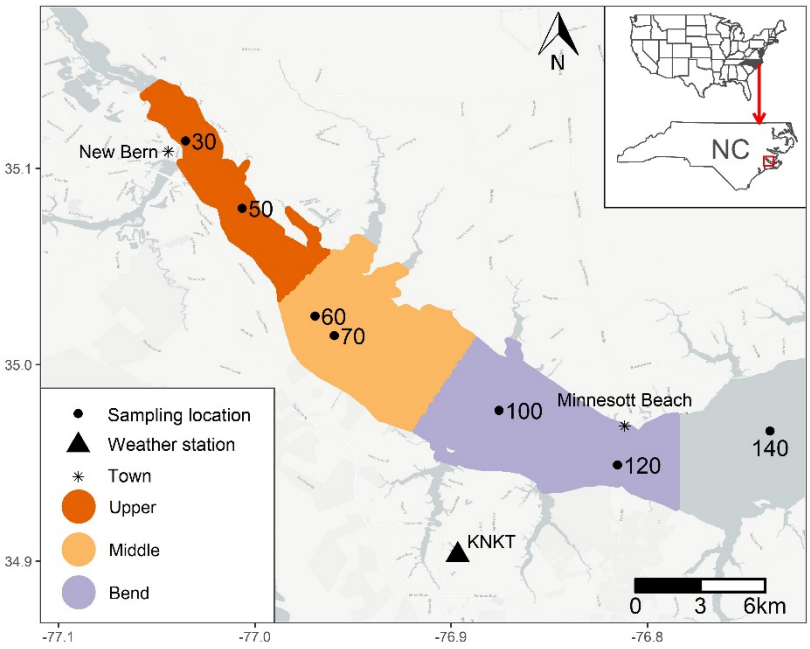

Fig. 1 Map of the Neuse Estuary study area, including the three modeled segments.

2.2 Piecewise regression

Piecewise regression (Model 1) was used to predict phytoplankton, expressed as chl-*a* (µg/L), as a function of riverine discharge, TN concentration, and temperature. Such a regression for the NRE was originally proposed by Borsuk et al. (2004), and we compare it to the more mechanistic models (Section 2.3). The relation of chl-*a* to discharge was addressed by a piecewise linear relationship (Faraway, 2015) with a breakpoint identified based on the magnitude of the flow (Paerl et al., 2014; Peierls et al., 2012). The response variable (chl-*a*) was log-transformed to

meet the assumption of the linear regression for normality of residuals. Flow was also log-transformed, though temperature and TN were left untransformed (Borsuk et al., 2004). Different averaging periods (1, 2, 10, 30, 60 d) for each predictor variable were tested based on predictive performance. The model intercept and coefficients for discharge and TN were allowed to vary hierarchically by segment (Gelman and Hill, 2007), while the temperature parameter was held constant across segments (based on preliminary analysis and to avoid over-fitting). Model 1 had the following form:

$$\ln(a_i) = \beta_{0,i} + \beta_{Q,l,i} \cdot \ln(Q) + \beta_{Q,h,i} \cdot (\ln(Q) - bp_i) \cdot d + \beta_{TN,i} \cdot TN + \beta_T \cdot T + \varepsilon_a \qquad (1)$$

where i represents model segments 1, 2, and 3 (upper, middle, and bend, respectively), a_i is chl-*a* concentration (μg/L), Q (m^3/d) is 2-day average river flow, TN (μg/L) is 10-day average riverine TN concentration, T (ºC) is water temperature. The coefficient β_0 (ln(μg/L)) is the intercept; $\beta_{Q,l}$ and $\beta_{Q,h}$ (ln(μg/L)/ln(m^3/d)) are coefficients for ln(Q) before and after breakpoint, respectively; β_{TN} (ln(μg/L)/(μg/L)) is the coefficient for TN; and β_T (ln(μg/L)/ºC) is the coefficient for T. In addition, bp (ln(m^3/d)) is the breakpoint and d is a binary variable associated with the breakpoint (d = 1, if ln(Q) > bp, otherwise d = 0). Finally, ε_a is the residual error, which is normally distributed on the ln scale.

2.3 Mechanistic models

Phytoplankton dynamics were represented by a parsimonious process-based biochemical model, where each segment was defined as a well-mixed reactor (Fig. 2). Model 2 included chl-*a*, non-algal organic matter (dissolved and particulate), and dissolved inorganic nitrogen (DIN) mass balances, while Model 3 additionally considered orthophosphate (OP). All mass balances were

represented via differential equations that were numerically solved using the LSODA algorithm (Soetaert et al., 2010) implemented via the 'odin' package in R (FitzJohn, 2019).

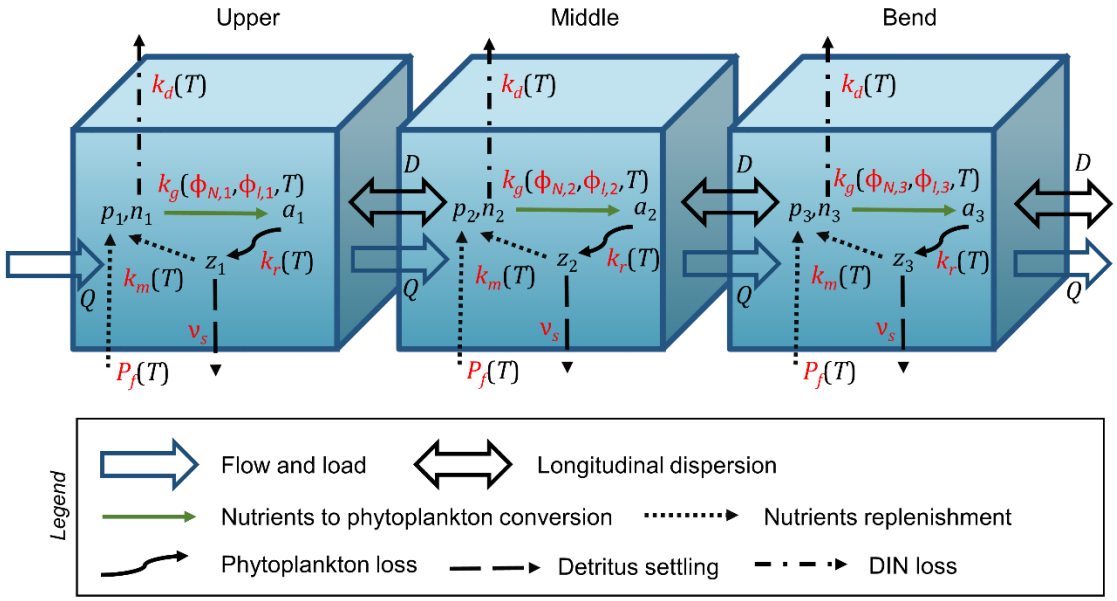

Fig. 2 Schematic representation of Model 3 as three longitudinal segments (upper, middle, and bend). Rubricated model parameters were calibrated within the Bayesian framework (Section 2.4). Symbols are described in the text and Table 1.

Chlorophyll-*a* concentration increases by means of photosynthetic growth associated with consumption of bioavailable nutrients, while chl-*a* decreases due to phytoplankton mortality. The differential equation for chl-*a* had the following form:

$$\frac{da_i}{dt} = (a_{i-1} - a_i) \cdot \frac{Q}{V_i} + k_g \cdot a_i \cdot \phi_{l,i} \cdot \phi_{N,i} \cdot \theta_g^{T-20} - k_r \cdot a_i \cdot \theta_r^{T-20} - \frac{D'_{i-1:i}}{V_i} \cdot (a_i - a_{i-1}) + \frac{D'_{i:i+1}}{V_i} \cdot (a_{i+1} - a_i) \quad (2)$$

where V_i (m^3) is volume (of segment i), Q (m^3/d) is flow, k_g (d^{-1}) is the maximum phytoplankton growth rate (at 20°C), k_r (d^{-1}) is the phytoplankton loss rate due to combined effect of respiration, excretion, and grazing. θ_g, and θ_r are temperature (T) adjustment parameters for k_g and k_r, respectively, and ϕ_N and ϕ_l are nutrient and light limitation factors described below. Parameter D' (m^3/d) is a bulk longitudinal dispersion coefficient (Chapra, 2008) estimated as in Katin et al. (2019).

Non-algal organic matter (detritus and zooplankton) in units of nitrogen (z, µg/L) increases due to phytoplankton mortality, and it decreases via mineralization or deposition to the sediment layer:

$$\frac{dz_i}{dt} = (z_{i-1} - z_i) \cdot \frac{Q}{V_i} + r_{na} \cdot k_r \cdot \theta_r^{T-20} \cdot a_i - \frac{\nu_s}{h_i} \cdot z_i - k_m \cdot z_i \cdot \theta_m^{T-20} - \frac{D'_{i-1:i}}{V_i} \cdot (z_i - z_{i-1}) + \frac{D'_{i:i+1}}{V_i} \cdot (z_{i+1} - z_i) \quad (3)$$

where h (m) is depth of the water column, r_{na} is the nitrogen-to-chl-a ratio, ν_s (m/d) is the settling velocity, k_m (d^{-1}) is the mineralization rate, and θ_m is a dimensionless temperature adjustment for k_m.

Bioavailable nutrients (DIN and OP) are delivered via riverine discharge, utilized by the phytoplankton for primary production, and are recycled back from the organic matter pool:

$$\frac{dx_i}{dt} = (x_{i-1} - x_i) \cdot \frac{Q}{V_i} - r_{xa} \cdot k_g \cdot a_i \cdot \phi_{l,i} \cdot \phi_{N,i} \cdot \theta_g^{T-20} + k_m \cdot r_{zx} \cdot z_i \cdot \theta_m^{T-20} - \frac{D'_{i-1:i}}{V_i} \cdot (x_i - x_{i-1}) + \frac{D'_{i:i+1}}{V_i} \cdot (x_{i+1} - x_i) + \Psi \quad (4)$$

where x is DIN (n, µg/L) or OP (p, µg/L), r_{xa} is the algal nitrogen- or phosphorus-to-chl-a ratio (r_{na} or r_{pa}), r_{zx} is the ratio of z to x (for n, $r_{zx} = 1$, for p, $r_{zx} = r_{pa} / r_{na}$), and Ψ is an additional source (+)

or sink (–) of x. For n, $\Psi = -k_d \cdot n \cdot \theta_d^{T-18.75}$ where k_d (d^{-1}) is the loss rate of DIN due to denitrification and other dissimilatory processes. For p, $\Psi = P_f \cdot \theta_p^{T-18.75} \cdot h^{-1}$, where P_f ($\mu g/m^2/d$) is the OP flux from the sediment. Note that 18.75 ºC is the mean NRE water temperature, and θ_d and θ_p are the associated temperature correction factors. While other types of nutrient fluxes (e.g., microbial N_2 fixation) may also occur in the estuary, they are not expected to be large enough to substantially influence model calibration and prediction (Affourtit et al., 2001; Spruill and Bratton, 2008; Whitall et al., 2003).

The phytoplankton growth rate was adjusted as a function of environmental conditions, including nutrient availability (ϕ_N) and light regime (ϕ_l). Nutrient limitation was represented by a Monod (1949) relationship, $\phi_N = x/(k_{sx}+x)$, where k_{sx} ($\mu g/L$) is the half saturation constant for nutrient x. For Model 2, nutrient limitation is based only on DIN (phosphorus is not modeled). For Model 3, nutrient limitation is based on a Liebig's law of the minimum, considering both DIN and OP, e.g. $\phi_N = min(\phi_n, \phi_p)$. Light limitation was represented using the Steele (1965) formulation, integrated over depth and time (eq. S4.1) following Chapra (2008). Daily values of the light extinction coefficient k_e (m^{-1}) required for ϕ_l estimation were determined via regressions with drivers of variability in optically active water quality constituents as explanatory variables. Chlorophyll *a* represented effects of absorbance by phytoplankton pigments, while 10-day natural log-transformed flow, 60-day temperature, and 2-day wind speed captured effects of season, flow, and resuspension on concentrations of chromophoric dissolved organic matter and suspended sediment (Section S4).

For the Upper segment, boundary conditions a_{i-1}, n_{i-1}, p_{i-1}, and z_{i-1} are riverine chl-*a*, DIN, OP, and non-algal organic matter concentrations, respectively. The latter term, z_{i-1}, consisted of dissolved and particulate organic nitrogen concentration exclusive of algal content, represented as

chl-*a* concentration multiplied by r_{xa}. For the lower Bend segment, boundary conditions a_{i+1}, n_{i+1}, p_{i+1}, and z_{i+1} were dynamically estimated based on empirical relationships between observations at downstream sampling location 140 (Fig. 1) and concentrations within the Middle and Bend segments (Section S2).

2.4 Model calibration and prior information

Bayesian calibration (i.e., parameter estimation) allows for derivation of posterior parameter distributions by systematically updating prior knowledge using the observed data through the likelihood function (Gelman et al., 2013). For all three models, the likelihood function was established assuming normally distributed uncorrelated error in the natural log-transformed space (Del Giudice et al., 2018; Ott, 1990). All three models were calibrated to observed chl-*a*. Model 2 was additionally calibrated to DIN, and Model 3 was additionally calibrated to DIN and OP. Bayesian inference was numerically implemented using Markov Chain Monte Carlo sampling. Specifically, Model 1 was calibrated using the 'RStan' package (Stan Development Team, 2016), which efficiently implements a Hamiltonian Monte Carlo sampling algorithm (Betancourt, 2017; Sorensen and Vasishth, 2015). For Models 2 and 3, an adaptive Metropolis sampling algorithm was adopted (Del Giudice et al., 2015; Haario et al., 2001; Malve et al., 2007), as it provided more flexibility for integrating the differential equation solver (Section 2.3). For each model, three parallel sampling chains were run at 30,000 iterations, with the first 10,000 discarded as burn-in, so that the posterior distributions are based on 60,000 posterior samples. Convergence was considered achieved when the square root of the ratio of total variance to within-chain variance was approximately equal to one for all parameters (Gelman et al., 2013).

The priors for the parameters were defined using normal (*N*) and truncated normal (*tN*) distributions. Truncated distributions prevented negative parameter values when they were mechanistically implausible. The parameters for Model 1 received weakly informative priors (Table S3.1). Prior information for mechanistic Models 2 and 3 were based on previous literature (Table 1).

Table 1 Prior parameters distributions for Models 2 (top 14) and 3 (all), derived from previous eutrophication studies in the NRE and elsewhere. Temperature corrections (θ) are associated with the preceding parameter.

Parameter	Description	Units	Prior	Literature
k_g	growth rate	d^{-1}	*tN*(1.0,0.3)	(Bowen and Hieronymus, 2000; Kruk et al., 2010; Lung and Paerl, 1988; Pinckney et al., 2001; Roelke, 2007)
θ_g	temperature correction	—	*tN*(1.07,0.03)	(Borsuk et al., 2004; Camacho et al., 2015; Peierls and Paerl, 2010)
r_{na}	ratio of *n* to *a*	μg*n*/μg*a*	*tN*(7.2,3)	(Chapra, 2008; Lung and Paerl, 1988)
k_{sn}	half-sat constant, *n*	μg/L	*tN*(20,5)	(Camacho et al., 2015; Chapra, 2008; Grover, 1989; Smayda, 1997)
k_r	loss rate	d^{-1}	*tN*(0.15,0.05)	(Chapra, 2008; EPA, 1985; Lung and Paerl, 1988; Ramin et al., 2011)
θ_r	temperature correction	—	*tN*(1.07,0.03)	(Borsuk et al., 2004; Camacho et al., 2015; Chapra, 2008)
k_m	recycling rate	d^{-1}	*tN*(0.15,0.05)	(Arhonditsis et al., 2008, 2007; Ramin et al., 2011)
θ_m	temperature correction	—	*tN*(1.07,0.03)	(Chapra, 2008; EPA, 1985; Liu et al., 2012; Rigosi et al., 2011)
ν_s	settling rate	m/d	*tN*(0.20,0.05)	(Arhonditsis et al., 2007; Lung and Paerl, 1988; Ramin et al., 2011)
I_s	optimal light level	W/m^2	*tN*(50,25)	(Boyer et al., 1994; Chapra, 2008; Edwards et al., 2016)
k_d	*n* removal rate	d^{-1}	*tN*(0.1,0.05)	(Fear et al., 2005; Ramin et al., 2011)
θ_d	temperature correction	—	*tN*(1,0.05)	(Fear et al., 2005; Khalil et al., 2018)
σ_n	residual SD for ln(*n*)	ln(μg/L)	*tN*(0,5)	—
σ_a	residual SD for ln(*a*)	ln(μg/L)	*tN*(0,1)	—
k_{sp}	half-sat constant, *p*	μg/L	*tN*(1.5,1)	(Camacho et al., 2015; Chapra, 2008; Grover, 1989; Smayda, 1997)
r_{pa}	ratio of *p* to *a*	g*p*/g*a*	*tN*(1,0.3)	(Lung and Paerl, 1988; Redfield et al., 1963)
P_f	sediment *p* flux	$\mu g/m^2/d$	*N*(744,400)	(Fear et al., 2004; Fisher et al., 1982)
θ_p	temperature correction	—	*tN*(1.08,0.05)	(Chapra, 2008)
σ_p	residual SD for ln(*p*)	ln(μg/L)	*tN*(0,1)	—

2.5 Models assessment, sensitivity, and scenario analysis

Models were assessed based on their predictive skill and realism of uncertainty quantification. Predictive skill was evaluated by root mean squared error (RMSE) and R^2, which represents the percent of the variance in the observations explained by the predictions (Faraway, 2015). For skill assessment, chl-*a* and nutrient predictions were obtained using the means of the Bayesian posterior parameter distributions and were compared to biweekly observations. Predictive performance was further assessed through a two-fold cross validation (Stone, 1974), where the first fold included 1997-2007 and the second fold consisted of 2008-2018 data. The portion of observations falling within the 90% cross-validated model predictive intervals were compiled to determine whether the model realistically characterizes uncertainty. Additionally, to assess the importance of riverine discharge, nutrient concentrations, and loadings, a sensitivity analysis was performed for Model 3 by adjusting these discharge and concentration values by +/−30%, and calculating the percent change of average chl-*a* across the simulation period.

All three models were used to screen the effect of changes in nutrient loading on mean chl-*a* under various hydrologic conditions and seasons. Scenarios were simulated by increasing or decreasing historical daily riverine nutrient concentrations (and thus loadings) by fixed percentages and re-running the model over the entire period of record. For the mechanistic models, the different forms of riverine (particulate plus dissolved) nutrient inputs (algal organic, non-algal organic, and inorganic) were reduced by the same percentage. For Model 3, we accounted for the fact that organic matter includes both nitrogen and phosphorus, and when only altering one nutrient at a time, the portion of the non-altered nutrient associated with the reduction in organic matter

was shifted to the inorganic pool. Hydrologic classifications were based on whether annual median flows fell into the lower (<61.2 m^3/d), middle (61.2-89.1 m^3/d), or upper (>89.1 m^3/d) third of historical flow conditions. Seasonal aggregations included winter (December – February), spring (March – May), summer (June – August), and fall (September – November).

3 Results and Discussion

3.1 Piecewise regression calibration (Model 1)

Piecewise regression parameter estimates quantify the effect of 2-day mean discharge, 10-day average TN concentration, and water temperature on chl-*a* (Fig. 3). Regression results confirm that chl-*a* has a nonlinear (breakpoint) relationship with river flow (Lucas et al., 2009; Peierls et al., 2012). Results indicate strong confidence (95% credible interval does not include zero) in the negative effect of discharge on chl-*a* at flows greater than the breakpoint ($\beta_{Q,h}$, Fig. 3, Table S3.2), likely representing the dominance of flushing over nutrient delivery and phytoplankton growth during high flows. On the other hand, discharge has a strong positive effect on chl-*a* at flows lower than the breakpoint for the Bend segment ($\beta_{Q,l}$), likely due to a shortage of bioavailable nutrients delivered downstream during low-flow conditions (Borsuk et al., 2004). Coefficients for discharge before the breakpoint ($\beta_{Q,l}$) for Upper and Middle segments include zero within 95% credible intervals ($\beta_{Q,l}$, Table S3.2), indicating a relatively weak relationship of chl-*a* with low flows. The estimated breakpoint (*bp*) increases downstream (Fig. 3), reflecting that higher discharges are needed for the effect of flushing to exceed the effect of increased nutrient delivery in segments with greater width and depth. Additionally, 95% credible intervals for (β_{TN}) imply that we have a strong degree of confidence in estimating the positive effect of riverine TN concentration on chl-*a* in the Middle and Bend segments of the estuary. These results are unique from Borsuk et al.

(2004), who found such relationships to be positive but insignificant for similar segments. Compared to previous studies that estimated significant (though not especially strong) positive relationships between temperature and chl-*a* (Borsuk et al., 2004; Hall et al., 2013), our regression results suggested weak water temperature effects on chl-*a* (Fig. 3, Table S3.2).

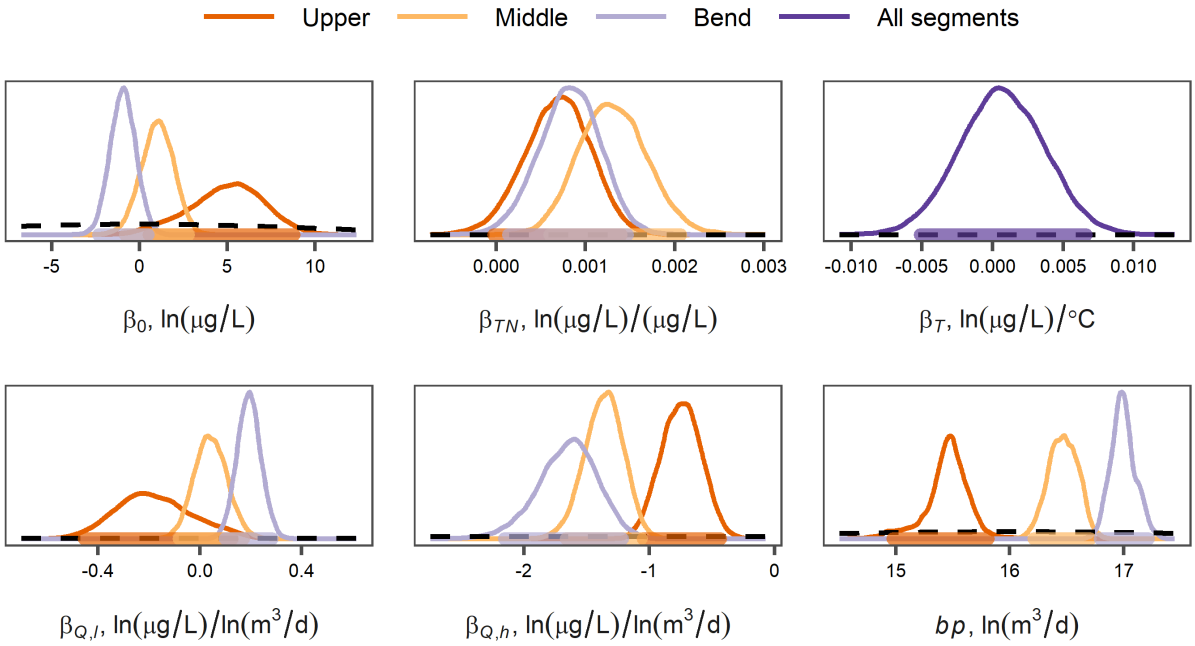

Fig. 3 Prior (dashed, black) and posterior (solid, with colors referring to segments) probability distributions for the deterministic parameters of Model 1. Horizontal bands indicate the 95% credible intervals of the marginal posterior distributions. Y-axis represents relative probability density. Parameter estimates are tabulated in Table S3.2.

3.2 Mechanistic model calibrations (Models 2 and 3)

Twelve and sixteen parameters are estimated through Bayesian inference for Models 2 and 3, respectively (Fig. 4, Table S3.2). In general, the posterior parameter estimates are

within the range of reported values from previous laboratory and modeling studies, consistent with the prior distributions (Table 1). Most marginal posterior distributions are narrower than the priors, indicating that the model formulations are suitable for updating the parameter values given the available calibration data. However, the posterior distribution of settling velocity (ν_s) is slightly wider than the prior for both formulations, and could perhaps be refined by calibrating to measures of non-algal organic matter in the estuary in future research.

The 95% credible intervals for the parameters of Model 3 typically overlap with those of Model 2, but there are some notable differences (Fig. 4). The estimates of phytoplankton growth (k_g) and loss (k_r) rates for Model 2 are greater than for Model 3. On the other hand, the best estimates of ratio of nitrogen to chl-*a* (r_{na}) and optimal light level (I_s) are smaller for Model 2 compared to Model 3. Interestingly, the estimate of r_{na} for Model 3 is higher than our prior, but close to values reported in other estuarine and coastal systems (Gowen et al., 1992; Li et al., 2010). While both models have similar predictive skill for chl-*a* and DIN (Section 3.4), differences in parameter estimates mentioned above indicate that the inclusion of phosphorus dynamics can substantially influence inference of mechanistic rates within a Bayesian framework. The posterior distributions also reveal substantial correlations among some parameters. For instance, phytoplankton growth rate (k_g) has a strong positive correlation ($r = 0.96$) with loss rate (k_r) indicating that an increase in one parameter can be largely compensated for by an increase in the other (see eq. 2). Additionally, phosphorus flux from the sediment (P_f) was negatively correlated with its temperature correction factor (θ_p, $r = -0.95$). However, despite these correlations, posterior distributions remain relatively tight when compared to the priors (Fig. 4).

The mechanistic models allow for an assessment of nutrient fluxes associated with (implicitly represented) sediment diagenesis and denitrification. Average flux of OP from the

sediments is 0.67 µg/L/d which is within the range of previously reported values for the NRE (Fear et al., 2004; Matson et al., 1983; Rizzo and Christian, 1996). Additionally, the high temperature correction coefficient, θ_p, (Fig. 4) suggests increased rates of phosphorus release from the sediment in summer compared to winter (mean fluxes are 1.87 and 0.01 µg/L/d, respectively), likely due to combined effects of high temperature and hypoxic conditions during summer (Cowan and Boynton, 1996; Fisher et al., 1982). Nitrogen removal rates from the water column are found to be 9.6 µg/L/d, which is consistent with previously estimated average denitrification rate for the NRE (8.7 µg/L/d) (Fear et al., 2005). This study confirms that dissimilatory nitrogen losses are lower in summer than in winter (mean fluxes are 7.34 and 22.6 µg/L/d, respectively), likely due to decreased DIN delivery (Fear et al., 2005; Piehler et al., 2002) and inhibited nitrification associated with oxygen deficits in summer (Hansen et al., 1981).

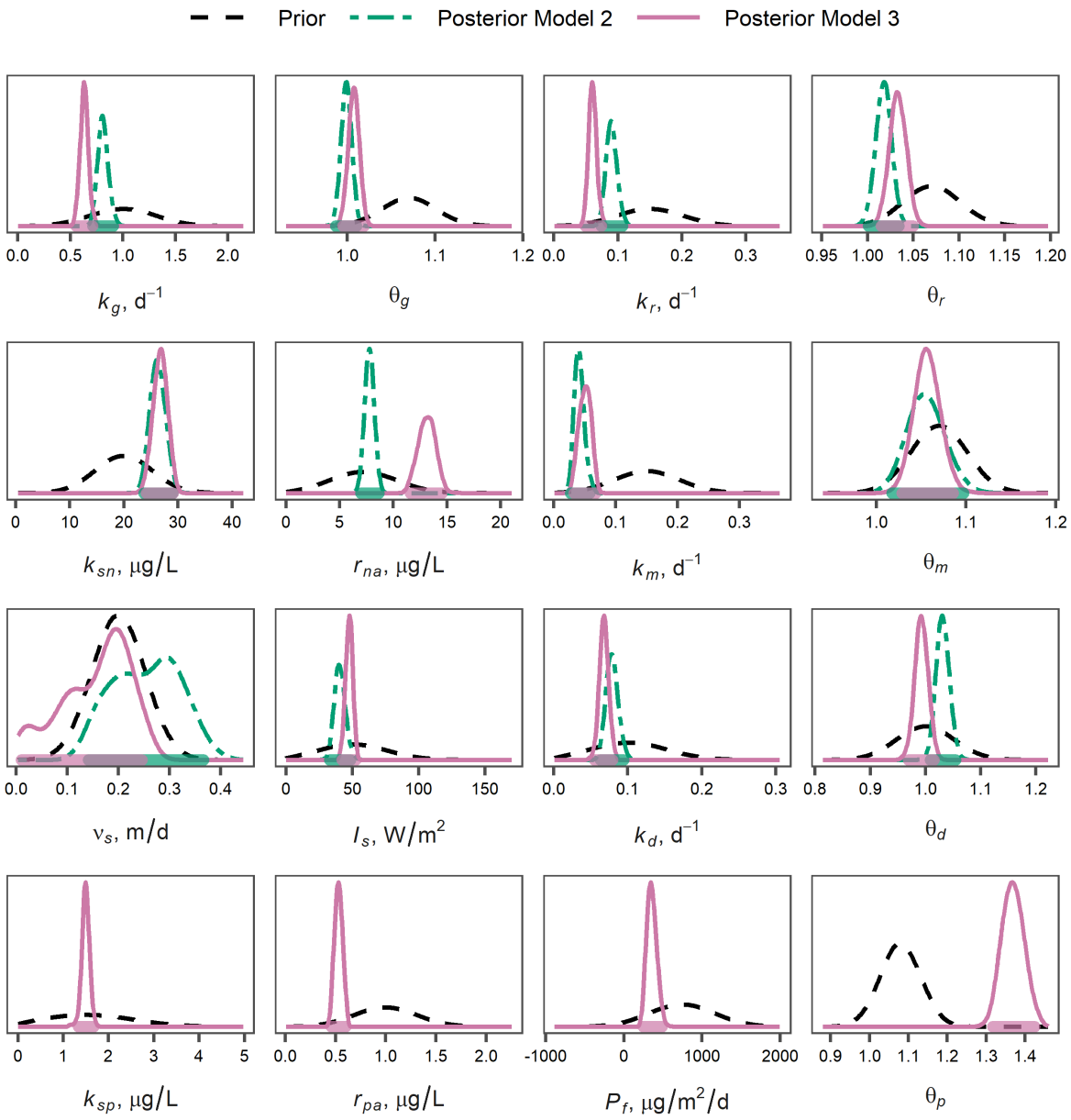

Fig. 4 Prior and posterior probability distributions for the calibrated deterministic parameters of Models 2 and 3. Horizontal bands indicate the 95% credible intervals of the marginal posterior parameter distributions. Y-axis represents relative probability density. Parameters are unitless unless indicated. Posterior parameter estimates are tabulated in Table S3.2.

3.3 Phytoplankton growth rate adjustment

The mechanistic models allow for exploring how temperature, light, and nutrient availability affect phytoplankton growth. Focusing on Model 3, the phytoplankton growth rate is reduced by 85%, on average, relative to the maximum growth rate at 20ºC (Fig. 5, black). These reductions are due to a combination of nutrient and light limitation, coupled with temperature adjustments.

Nutrient limitation, ϕ_N, is more influential in summer and less strong in winter, reducing average growth rates by 42% and 21% in these seasons, respectively (Fig. 5, orange). It is notable that nutrient limitation of phytoplankton growth has the greatest environmental (i.e., temporal) variability compared to temperature and light effects (Fig. 5). As riverine nutrients are consumed by phytoplankton, results indicate that substantial nutrient limitation (i.e., $\phi_N < 0.83$; Chapra, 2008) increases moving down the estuary, occurring 41%, 68%, and 74% of the time for Upper, Middle and Bend segments (Fig. 6). We also see that nutrient limitation is most severe under dry (i.e., low river flow) conditions, even in winter months (Fig. 6).

Nitrogen is the main nutrient limiting phytoplankton production in the NRE; about 60% of the time based on Model 3, which is consistent with previous studies for this estuary (Cira et al., 2016; Paerl et al., 1995; Pinckney et al., 2001; Rudek et al., 1991) and the general concept of nitrogen limitation in estuarine and coastal waters (Nixon, 1995; Howarth and Marino, 2006). Phosphorus is found to limit primary production only about 1.3% of the time (107 d over almost 22 years) in any segment over two decades. These rare phosphorus-limitation events occurred mostly in the Upper segment in late winter and early spring (Fig. 6) when TP loadings were substantially depressed. These results agree well with previous experimental findings for the NRE that showed occasional phosphorus controls on chl-*a* production that occurred only in late winter

and early spring (Pinckney et al., 1999; Rudek et al., 1991). Expectedly, if riverine TP concentration is reduced by 30% in the model, phosphorus limitation becomes more pronounced, occurring 15% of the time, but nitrogen remains the key nutrient, limiting phytoplankton growth 46% of the time. These results are consistent with findings from both the Gulf of Mexico (Fennel and Laurent, 2018) and Chesapeake Bay (Malone et al., 1996), which defined nitrogen as the major limiting nutrient and phosphorus occasionally limiting in spring and early summer.

Light availability in this turbid estuary is also a major regulator of phytoplankton growth, reducing it on average by 77% (Fig. 2.5, yellow), though part of this is simply attributable to the sun being down 50% of the time (at night), on average (Section S2.4). The additional light limitation (27%) occurs due to light attenuation in the atmosphere (e.g., cloud cover) and water column. These results are generally consistent with previous estuarine studies that outlined the importance of light in influencing primary productivity (Gameiro et al., 2011; Pennock and Sharp, 1992). Factors affecting the water column light extinction coefficient (k_e) were estimated via Bayesian regression (Section S4, eq. S4.5). Results from this regression quantify how algal accumulation (chl-*a*) increases light extinction, while background attenuation decreases moving down the estuary, presumably due to the settling of suspended material and the dilution, degradation, and flocculation of chromophoric dissolved organic matter (Vähätalo and Zepp, 2005). Background attenuation is also strongly related to riverine discharge (natural log-transformed discharge alone explains 36% of variability in light extinction coefficient), which is typical for a river-dominated estuary (Bowen and Hieronymus, 2003; McSweeney et al., 2017).

Temperature only slightly influences growth rate in the mechanistic model. In Model 3, temperature enhances summer growth by 5% and decreases growth rate in winter by 6% relative to the maximum growth rate at 20ºC (Fig. 5, red). Overall, the temperature effects observed in this

study (all models) are smaller than those reported in the previous studies (Table 2.1). A possible explanation for this discrepancy may be that different phytoplankton populations have various optimal temperatures, consistent with observed blooms of specific taxa occurring throughout the year (Pinckney et al., 1998). Finally, the estimated temperature adjustments may reflect additional drivers of seasonal variability (e.g., vertical stratification) or changes in grazer communities that are not explicitly accounted for in the model (Wetz et al., 2011).

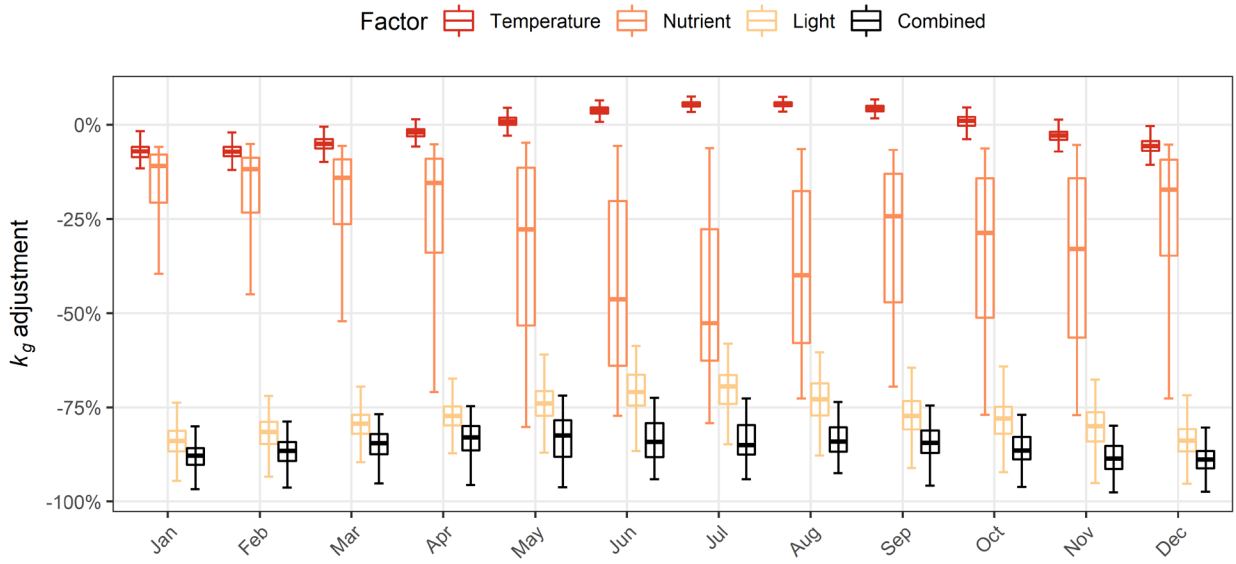

Fig. 5 Monthly adjustment of calibrated phytoplankton growth rate at 20ºC ($k_g = 0.64$ d^{-1}) to temperature, nutrients, light, and all three factors combined. Results are from Model 3 and averaged across all three segments. Environmental variability is represented by the boxes showing interquartile range, while center line is the median. Whiskers extend to the extreme value or 1.5 times the interquartile range (whichever is less).

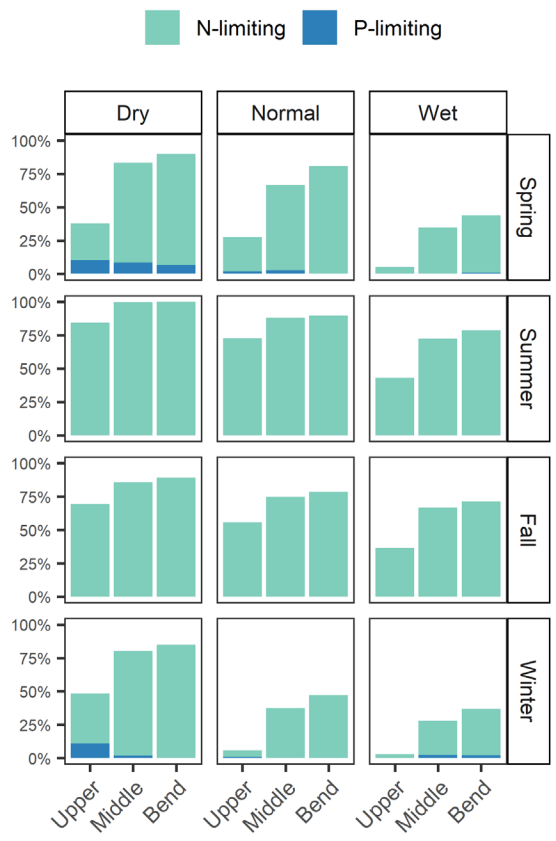

Fig. 6 Percent of time when nitrogen or phosphorus limitation occurs in the Upper, Middle, and Bend segments, shown for different hydrologic regimes and seasons (Model 3). Note that nutrient limitation is considered to occur when either DIN or OP is less than five times their respective Monod half saturation constants (Chapra, 2008).

3.4 Model predictive skill

Overall, Models 1, 2, and 3 explain 43%, 38%, and 38% of variability in log-transformed chl-*a*, respectively, across all seasons and segments (Fig. 7 top row, Table S5) with corresponding RMSEs of 0.65, 0.68, and 0.67 ln(µg/L). For comparison, cross-validated Models 1, 2, and 3 explain 37%, 36%, and 35% of variability in log-transformed observed chl-*a*, respectively, with corresponding RMSEs of 0.68, 0.69, and 0.70 ln(µg/L). The larger drop in performance for

Model 1 (i.e., R^2 of 43% drops to 37% in cross validation) suggests it is less robust, though it still slightly outperforms the mechanistic models. In cross validation, 11.4%, 20.5%, and 18.5% of the observations fall outside of the 90% prediction intervals for Models 1, 2, and 3, respectively, indicating the models somewhat underrepresent forecasting uncertainty. In general, uncertainties may be underestimated due to temporal autocorrelation among the biweekly samples (e.g., Fig. S5), which could be a subject for future model improvement (Reichert and Mieleitner, 2009).

Consistent with results from previous studies, performances decline moving downstream for all models (Table S5), likely due to diminishing hydrologic forcing (Borsuk et al., 2003; Bowen and Hieronymus, 2003; Wool et al., 2003) and less variability in chl-*a* observations (standard deviations of 1.0, 0.78 and 0.69 ln(μg/L) for Upper, Middle, and Bend segments, respectively) that can reduce the signal to noise ratio of the data. Interestingly, the mechanistic models perform better than the statistical model in the Middle segment but worse in the Upper and Bend segments (Table S5). It is important to note that Models 2 and 3 were also calibrated to bioavailable nutrients, with both models explaining 64% of variability in DIN, and Model 3 additionally explaining 56% of variability in OP (Fig. 7).

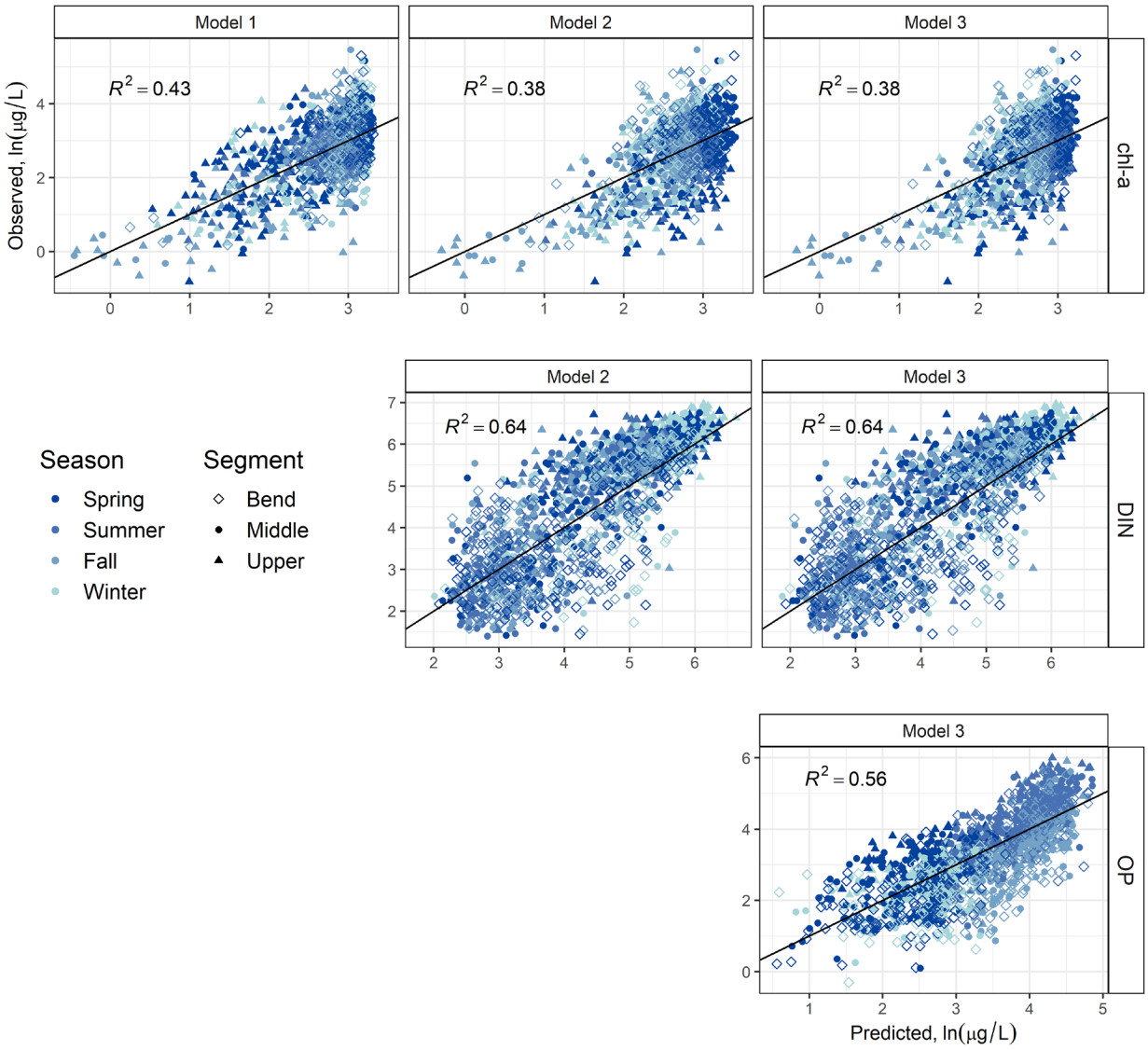

Fig. 7 Observed versus predicted natural log-transformed chl-*a* (top row), DIN (middle row) and OP (bottom row) concentrations for 22-year study period for the three models. Black diagonals represent the 1:1 line (i.e., line of perfect prediction).

3.5 Sensitivity to riverine inputs

River discharge influences residence time, nutrient delivery, and light availability in estuarine systems (Abreu et al., 2010; Cloern, 2001; Liu et al., 2018; Wang et al., 2019). Previous NRE studies outlined the role of riverine inputs in controlling estuarine algal biomass and composition (Borsuk et al., 2004; Hall et al., 2013; Peierls et al., 2012), but have not isolated and quantified chl-*a* responses to changes in discharge, concentration, and loading. Here, sensitivity analysis (based on Model 3) focused on changing flows and loadings +/−30%. While riverine inputs have considerable interannual variability, we assumed +/−30% represents a reasonable long-term response due to changes in climate and anthropogenic watershed activities, and it is also consistent with TMDL reduction target (NCDWQ, 2001). From this analysis, the greatest increase in chl-*a* (+18.3% across segments, Table 2, case E) occurs when flow is reduced by 30% and loading is held constant, such that riverine nutrient concentrations increase by 43%. Conversely, a large chl-*a* reduction in the Upper segment (−17.6%, case F) occurs when flow is increased by 30% and loading is held constant. However, for the Middle and Bend segments, the greatest chl-*a* reductions are in response to 30% riverine concentration and loading reductions (with flows held constant, case C).

Congruent changes in river flow and load (Table 2, cases A and B), such that nutrient concentrations remained the same, had relatively little impact on chl-*a* concentrations. However, it is noteworthy that for both cases A and B, the effect on chl-*a* in the Bend segment is almost the same (a small reduction). Here, when flows and loadings are reduced by 30%, less nutrients reach this downstream segment, but when flows and loadings are increased 30%, the effects of flushing over-compensates for the increased nutrient loading. These results indicate that current flow rates provide near-optimal conditions for chl-*a* accumulation in the Bend segment. At the same time,

we note that the largely negative relationships between flow and chl-*a* (considering all segments) are coherent with a recent hypoxia study, which indicated the important role of winter discharge in flushing biomass and diminishing deposition of organic matter to the sediments (Katin et al., 2019).

Overall, these results provide a mechanistic quantification of how freshwater inputs have a strong and multifaceted effect on phytoplankton production and water quality in the NRE (Paerl et al., 2014; Peierls et al., 2012; Pinckney et al., 1999). From a watershed management perspective, these results highlight the importance of controlling dry weather loads (e.g., point sources, leaking animal wastes), which can lead to high riverine nutrient concentrations in dry years (Alameddine et al., 2011; Strickling and Obenour, 2018). Such a scenario is approximately analogous to case E (Table 2).

Table 2 Percent change in chl-*a* for Upper, Middle, Bend, and overall NRE, relative to average baseline concentrations of 14.3, 16.4, 16.6, and 15.8 μg/L, respectively. Estuary response are shown based on sensitivity-analysis adjustments to riverine discharge (*Q*), riverine TN and TP loadings (*L*), and concentrations (*c*). The largest (positive and negative) changes in chl-*a* are highlighted in bold. All results are based on Model 3.

case	input variation			segment response			overall response
	Q	*L*	*c*	Upper	Middle	Bend	
A	−30%	−30%	−	4.3%	0.4%	−0.5%	1.3%
B	+30%	+30%	−	−4.6%	−1.7%	−0.8%	−2.3%
C	−	−30%	−30%	−16.6%	**−13.8%**	**−11.5%**	**−13.8%**
D	−	+30%	+30%	16.0%	13.3%	11.0%	13.3%
E	−30%	0%	+43%	**25.5%**	**17.2%**	**13.2%**	**18.3%**
F	+30%	0%	−23%	**−17.6%**	−12.9%	−10.2%	−13.4%

3.6 Nutrient loading scenarios

Because watershed nutrient loading is the most management-relevant estuary input, we compare estuary chl-*a* responses to a range of loading adjustments using all three models (Fig. 8). All models indicate that chl-*a* is responsive to reductions in riverine TN load and concentration (flow is held constant). For instance, a 30% TN loading reduction will result in 26.0%, 16.1% and 13.7% decrease in average chl-*a* concentrations for Models 1, 2, and 3, respectively. On the other hand, these models suggest that a 30% increase in TN loadings will result in 38.3%, 15.6% and 12.2% rises in chl-*a*, respectively. Thus, Model 1 is most responsive, averaging a 10.4% chl-*a* adjustment for each 10% TN change. We note that the magnitude of this response could be partially related to the transformations used in the regression (natural log for chl-*a*, but no transformation for TN), which were applied consistent with Borsuk et al. (2004). Interestingly, the Model 1 responses are somewhat similar to those documented for the nearby New River Estuary (NC), where statistical analyses of observed data indicated that each 10% reduction in total nutrients would decrease chl-*a* by 13.2% (Mallin et al., 2005). However, from a more mechanistic perspective, it is unclear how the ratio of % change in chl-*a* to nutrients could exceed 1:1 based on stoichiometric considerations (Chapra, 2008). Furthermore, negative feedbacks, such as increased algal biomass leading to more light extinction, would suggest ratios of less than 1:1. Consistent with these mechanistic considerations, Models 2 and 3 indicate smaller responses to loading perturbations, where chl-*a* is altered 5.3% and 4.3%, respectively, for each 10% TN loading change. These mechanistic model results broadly support previous NRE studies, which indicated 4.4% (Borsuk et al., 2002), 5.1% (Bowen and Hieronymus, 2003), 4.9% (Wool et al., 2003) reductions in chl-*a* to similar TN reductions. It is also worthwhile to compare with other systems

like Tampa Bay, where each 10% TN loading reduction resulted in about a 6.7% decrease in chl-*a* (Greening and Janicki, 2006).

Additionally, Model 3 is used to investigate how simultaneous nitrogen and phosphorus loading modifications affect chl-*a* levels. When riverine TN and TP are altered by 10%, chl-*a* changes by 4.6% (Fig. 8), compared to a 4.3% response when altering TN only. This result is generally consistent with a study in Boston Harbor, where a 10% TN loading reduction with parallel 11.3% TP reduction helped to reduce chl-*a* by 3.5% (Taylor et al., 2011). If solely TP is reduced by 10% or 30%, then chl-*a* is expected to decrease by just 0.3% or 2.4%, respectively (averaged across all segments). Interestingly, if sediment phosphorus (P_f) flux is reduced proportionally to TP load, there is little additional reduction in chl-*a* (<1%). While these results suggest that nitrogen controls alone are nearly as effective as combined nitrogen and phosphorus control, we caution that reducing just one nutrient may produce undesirable shifts in phytoplankton community composition (Berthold et al., 2018; Kelly et al., 2019; Paerl et al., 2016) or the location of algal blooms in the estuary (Paerl et al., 2004). Thus, parallel nitrogen and phosphorus controls should be considered for long-term NRE eutrophication management.

Seasonally, the statistical model (Model 1) does not exhibit diverse responses to nutrient loading (Fig. 8). In Model 1, seasonality is primarily represented by temperature via coefficient β_T, which largely overlaps zero (Fig. 4). However, the mechanistic models indicate larger responses of chl-*a* to loading changes in the spring, particularly under dry conditions (Fig. 8). Across hydrologic conditions, a 30% change in nutrient loading will result in 17.9%, 12.8%, 10.5%, and 13.5% changes in chl-*a* in spring, summer, fall, and winter, respectively. The periods with greater chl-*a* responses are generally those with higher flows and nutrient loadings.

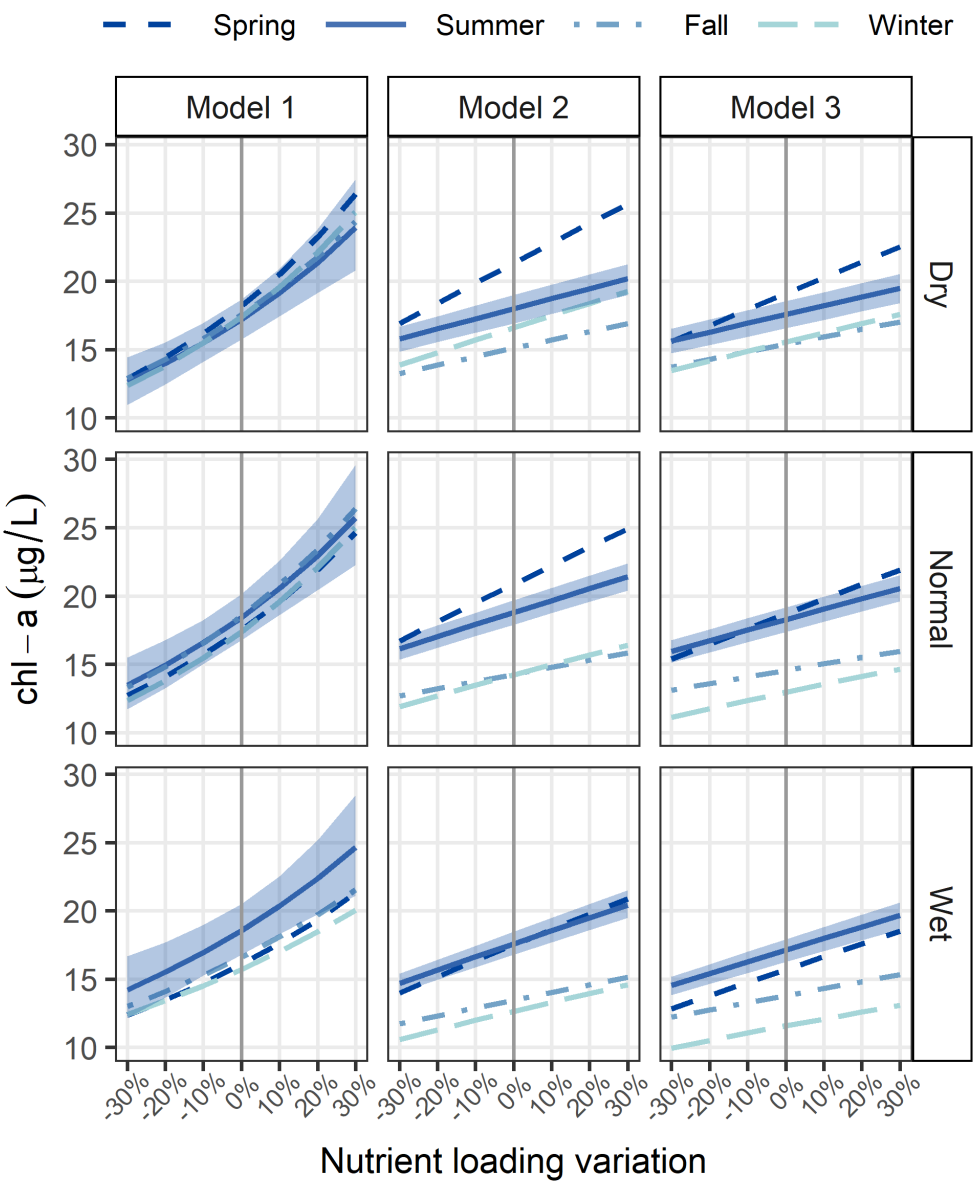

Fig. 8 Average chl-*a* predictions across all segments from Models 1, 2, and 3 shown for four seasons and three hydrologic conditions under various TN loading adjustments (TN and TP in the case of Model 3). Loading scenarios are based on modifying riverine incoming nutrient concentrations by the percent shown; flows and other model inputs are held constant. For clarity, 90% credible intervals are shown only for summer scenarios (blue ribbon).

Another way of assessing the influence of riverine nutrients on chl-*a* is by focusing on the probability of chl-*a* exceeding the State criterion of 40 μg/L. For instance, a 30% reduction in TN and TP would help to reduce the probability of chl-*a* violating the criterion in Middle and Bend segments from 11% to 8%, which is less than the 10% exceeded rate allowed by NC water quality criteria (Fig. S6). Thus, this study implies a smaller loading reduction than Borsuk et al. (2003), which suggested a 45% reduction was needed. However, it should be noted that the study period (1997-2018) has a 7% lower average riverine TN concentration than the baseline period (1998-2000) used for previous NRE assessments (Stow et al., 2003).

3.7 Bayesian approach and model comparison

This study advances the development of statistical and mechanistic water quality models for river-dominated estuarine systems within the Bayesian framework. While piecewise regression (Model 1) is based on relatively simple empirical relationships drawing on previous modeling efforts, this is the first time the approach has been embedded in a Bayesian hierarchical framework. Moreover, Models 2 and 3 expand the spatio-temporal scope of Bayesian mechanistic phytoplankton modeling relative to previous studies (Parslow et al., 2013; Ramin et al., 2011) by simulating chl-*a* dynamics over multiple decades and across a longitudinally segmented waterbody. The models were designed to be computationally efficient, allowing us to obtain daily simulations over almost 22 years quickly (i.e., less than 4 s), which facilitates the MCMC approach to Bayesian inference. Within the Bayesian framework, model parameters are informed by a combination of prior literature findings and the multi-decadal calibration data, enabling systematic parameter estimation and uncertainty quantification (Beck, 1987; Ganju et al., 2016).

However, both types of models possess limitations, including coarse spatial resolution and simple or implicit representation of certain processes (e.g. sediment diagenesis, denitrification). Furthermore, the model represents grazing as a simple first-order loss rate, without consideration of more complex trophodynamics (Kimmel et al., 2015). Even given these limitations, all three models explain a substantial portion of longitudinal variability in natural log-transformed chl-*a* in the NRE ($R^2 > 0.35$, Section 3.4). Unexplained variability in chl-*a* might be due to factors beyond model structure, including erratic bloom-forming phytoplankton taxa (Paerl et al., 2018a, 2014; Pinckney et al., 1998), the spatial patchiness of biomass (Hall et al., 2013), and variable ratios of chl-*a* to nutrients (Geider et al., 1997; Jakobsen and Markager, 2016). Additionally, the cross-validation RMSEs of all three models (Table S5, average of 0.69 ln(µg/L)) suggest favorable predictive performance when compared to previous NRE modeling studies with average RMSE of 0.86 ln(µg/L) (Stow et al., 2003).

Model 1 performs similar to the mechanistic Models 2 and 3 for the prediction of chl-*a* when subject to cross validation (Section 3.4). Thus, the piecewise regression provides a relatively simple and computationally efficient approach to forecasting algal levels. At the same time, mechanistic Models 2 and 3 integrate over a wider range of biogeochemical processes and are simultaneously calibrated to bioavailable nutrients, explaining the majority ($R^2 > 0.5$) of variability in DIN and OP (Fig. 7). Also, parameters in the mechanistic models have physical meaning and can be readily informed based on prior information, which promotes a realistic representation of biophysical relationships and relatively robust predictive performance based on cross validation, consistent with another recent phytoplankton model comparison study (Han et al., 2021). Additionally, the mechanistic models lead to more realistic load reductions scenarios, as described in Section 3.6, with substantially reduced uncertainty (i.e., credible intervals, Fig. 8). Thus, the

mechanistic models appear advantageous when predicting the response of the estuary to major changes in riverine inputs.

4 Conclusions

In this study, we compared empirical and mechanistic phytoplankton modeling approaches to evaluate how hydrologic forcings and nutrient limitation govern eutrophication in a shallow estuary. We developed these approaches using Bayesian inference, which assimilates prior knowledge and calibration data to provide probabilistic parameter estimates and water quality predictions. The resulting models characterize the role of riverine inputs and indicate that nutrient concentration reductions, due to either increased flow dilution or reduced load, are the key to reducing algal levels in the estuary. Although the purely statistical model had slightly higher predictive skill for chl-*a*, the mechanistic approach allows for a more thorough assessment of controls on algal productivity, simulation of nutrients, and more realistic scenario forecasts with reduced uncertainties. Additionally, mechanistic model results suggest that nutrient limitation of algal growth is dominated by nitrogen, rather than phosphorus, even in the upstream (less-saline) portion of the study area. Overall, the mechanistic models appear more useful for evaluating the hypothetical nutrient loading scenarios and for providing multifaceted support of management decisions. Finally, model results suggest that achievement of the current nutrient reduction goal (30% TN reduction) will most likely facilitate compliance with NC criteria, based on the frequency of exceeding high chl-*a* (40 µg/L) concentrations. The Bayesian mechanistic approach developed here can be transferred to other river-dominated estuaries, and the posterior parameter distributions from this study can potentially inform prior distributions for future models of less monitored systems.

Acknowledgments

We are grateful to Dr. Ryan Paerl and two anonymous reviewers for their valuable suggestions on the manuscript. This research was funded by NC Sea Grant (Project 2016-R/16-HCE-1), and data were made available through the Neuse River Modeling and Monitoring Program, ModMon, which was supported by the NC Department of Environmental Quality and National Fish and Wildlife Foundation (Grant 8020.16.053916). The authors have no financial conflicts of interest to disclose.

References

Abreu, P.C., Bergesch, M., Proença, L.A., Garcia, C.A.E., Odebrecht, C., 2010. Short- and Long-Term Chlorophyll a Variability in the Shallow Microtidal Patos Lagoon Estuary, Southern Brazil. Estuaries and Coasts 33, 554–569. https://doi.org/10.1007/s12237-009-9181-9

Affourtit, J., Zehr, J.P., Paerl, H.W., 2001. Distribution of nitrogen-fixing microorganisms along the Neuse River Estuary, North Carolina. Microb. Ecol. 41, 114–123. https://doi.org/10.1007/s002480000090

Alameddine, I., Qian, S.S., Reckhow, K.H., 2011. A Bayesian changepoint-threshold model to examine the effect of TMDL implementation on the flow-nitrogen concentration relationship in the Neuse River basin. Water Res. 45, 51–62. https://doi.org/10.1016/j.watres.2010.08.003

Arhonditsis, G.B., Papantou, D., Zhang, W., Perhar, G., Massos, E., Shi, M., 2008. Bayesian calibration of mechanistic aquatic biogeochemical models and benefits for environmental management. J. Mar. Syst. 73, 8–30. https://doi.org/10.1016/j.jmarsys.2007.07.004

Arhonditsis, G.B., Qian, S.S., Stow, C.A., Lamon, E.C., Reckhow, K.H., 2007. Eutrophication risk assessment using Bayesian calibration of process-based models: Application to a mesotrophic lake. Ecol. Modell. 208, 215–229. https://doi.org/https://doi.org/10.1016/j.ecolmodel.2007.05.020

Bales, J.D., Robbins, J.C., 1999. A Dynamic Water-Quality Modeling Framework for the Neuse River Estuary, North Carolina, U.S. Geological Survey Water-Resources Investigations Report.

Beck, M.B., 1987. Water quality modeling: A review of the analysis of uncertainty. Water Resour. Res. 23, 1393–1442. https://doi.org/10.1029/WR023i008p01393

Berthold, M., Karsten, U., von Weber, M., Bachor, A., Schumann, R., 2018. Phytoplankton can bypass nutrient reductions in eutrophic coastal water bodies. Ambio 47, 146–158. https://doi.org/10.1007/s13280-017-0980-0

Betancourt, M., 2017. A Conceptual Introduction to Hamiltonian Monte Carlo.

Borsuk, M.E., Higdon, D., Stow, C.A., Reckhow, K.H., 2001. A Bayesian hierarchical model to predict benthic oxygen demand from organic matter loading in estuaries and coastal zones. Ecol. Modell. 143, 165–181. https://doi.org/10.1016/S0304-3800(01)00328-3

Borsuk, M.E., Stow, C.A., Reckhow, K.H., 2004. Confounding Effect of Flow on Estuarine Response to Nitrogen Loading. J. Environ. Eng. 130, 605–614. https://doi.org/10.1061/(ASCE)0733-9372(2004)130:6(605)

Borsuk, M.E., Stow, C.A., Reckhow, K.H., 2003. Integrated Approach to Total Maximum Daily Load Development for Neuse River Estuary using Bayesian Probability Network Model (Neu-BERN). J. Water Resour. Plan. Manag. 129, 271–282. https://doi.org/10.1061/(ASCE)0733-9496(2003)129:4(271)

Borsuk, M.E., Stow, C.A., Reckhow, K.H., 2002. Predicting the Frequency of Water Quality Standard Violations: A Probabilistic Approach for TMDL Development. Environ. Sci. Technol. 36, 2109–2115. https://doi.org/10.1021/es011246m

Bowen, J.D., Hieronymus, J., 2000. Neuse River Estuary modeling and monitoring stage 1: Predictions and uncertainty analysis of response to nutrient loading using a mechanistic eutrophication model. Water Resources Research Institute of the University of North Carolina (WRRI), Report No. 325-D.

Bowen, J.D., Hieronymus, J.W., 2003. A CE-QUAL-W2 Model of Neuse Estuary for Total

Maximum Daily Load Development. J. Water Resour. Plan. Manag. 129, 283–294. https://doi.org/10.1061/(ASCE)0733-9496(2003)129:4(283)
Boyer, J.N., Stanley, D.W., Christian, R.R., 1994. Dynamics of NH4 + and NO3 − uptake in the water column of the Neuse River Estuary, North Carolina. Estuaries 17, 361–371. https://doi.org/10.2307/1352669
Bricker, S.B., Clement, Christopher G. Pirhalla, D.E., Orlando, S.P., Farrow, D.R.G., 1999. National Estuarine Eutrophication Assessment: Effects of Nutrient Enrichment in the Nation's Estuaries. Silver Spring, MD.
Camacho, R.A., Martin, J.L., Watson, B., Paul, M.J., Zheng, L., Stribling, J.B., 2015. Modeling the Factors Controlling Phytoplankton in the St. Louis Bay Estuary, Mississippi and Evaluating Estuarine Responses to Nutrient Load Modifications. J. Environ. Eng. 141, 04014067. https://doi.org/10.1061/(ASCE)EE.1943-7870.0000892
Chapra, S., 2008. Surface Water-Quality Modeling. Waveland Press, Inc.
Cira, E.K., Paerl, H.W., Wetz, M.S., 2016. Effects of Nitrogen Availability and Form on Phytoplankton Growth in a Eutrophied Estuary (Neuse River Estuary, NC, USA). PLoS One 11, e0160663. https://doi.org/10.1371/journal.pone.0160663
Cloern, J.E., 2001. Our evolving conceptual model of the coastal eutrophication problem. Mar. Ecol. Prog. Ser. 210, 223–253.
Cowan, J.L.W., Boynton, W.R., 1996. Sediment-Water Oxygen and Nutrient Exchanges along the Longitudinal Axis of Chesapeake Bay: Seasonal Patterns, Controlling Factors and Ecological Significance. Estuaries 19, 562. https://doi.org/10.2307/1352518
de Jonge, V.N., Elliott, M., Orive, E., 2002. Causes, historical development, effects and future challenges of a common environmental problem: eutrophication. Hydrobiologia 475, 1–19. https://doi.org/10.1023/A:1020366418295
Deamer, N., 2009. Neuse River Basinwide Water Quality Plan. NC Department of Environment and Natural Resources, Raleigh.
Del Giudice, D., Fang, S., Scavia, D., Davis, T.W., Evans, M.A., Obenour, D.R., 2021. Elucidating controls on cyanobacteria bloom timing and intensity via Bayesian mechanistic modeling. Sci. Total Environ. 755, 142487. https://doi.org/10.1016/j.scitotenv.2020.142487
Del Giudice, D., Muenich, R.L., Kalcic, M.M., Bosch, N.S., Scavia, D., Michalak, A.M., 2018. On the practical usefulness of least squares for assessing uncertainty in hydrologic and water quality predictions. Environ. Model. Softw. 105, 286–295. https://doi.org/10.1016/j.envsoft.2018.03.009
Del Giudice, D., Reichert, P., Bareš, V., Albert, C., Rieckermann, J., 2015. Model bias and complexity – Understanding the effects of structural deficits and input errors on runoff predictions. Environ. Model. Softw. 64, 205–214. https://doi.org/10.1016/j.envsoft.2014.11.006
Eby, L.A., Crowder, L.B., 2002. Hypoxia-based habitat compression in the Neuse River Estuary: context-dependent shifts in behavioral avoidance thresholds. Can. J. Fish. Aquat. Sci. 59, 952–965. https://doi.org/10.1139/f02-067
Edwards, K.F., Thomas, M.K., Klausmeier, C.A., Litchman, E., 2016. Phytoplankton growth and the interaction of light and temperature: A synthesis at the species and community level. Limnol. Oceanogr. 61, 1232–1244. https://doi.org/10.1002/lno.10282
EPA, 1985. Rates, constants, and kinetics formulations in surface water quality modeling, 2nd ed, United States Environmental Research And Protection Laboratory Agency. United States Environmental Protection Agency, Office of Research and Development, Environmental

Research Laboratory.
Faraway, J.J., 2015. Linear Models with R, 2nd ed. Taylor & Francis Group.
Fear, J., Gallo, T., Hall, N., Loftin, J., Paerl, H., 2004. Predicting benthic microalgal oxygen and nutrient flux responses to a nutrient reduction management strategy for the eutrophic Neuse River Estuary, North Carolina, USA. Estuar. Coast. Shelf Sci. 61, 491–506. https://doi.org/10.1016/j.ecss.2004.06.013
Fear, J.M., Thompson, S.P., Gallo, T.E., Paerl, H.W., 2005. Denitrification rates measured along a salinity gradient in the eutrophic Neuse River estuary, North Carolina, USA. Estuaries 28, 608–619. https://doi.org/10.1007/BF02696071
Fennel, K., Laurent, A., 2018. N and P as ultimate and proximate limiting nutrients in the northern Gulf of Mexico: implications for hypoxia reduction strategies. Biogeosciences 15, 3121–3131. https://doi.org/10.5194/bg-15-3121-2018
Fiechter, J., Herbei, R., Leeds, W., Brown, J., Milliff, R., Wikle, C., Moore, A., Powell, T., 2013. A Bayesian parameter estimation method applied to a marine ecosystem model for the coastal Gulf of Alaska. Ecol. Modell. 258, 122–133. https://doi.org/10.1016/j.ecolmodel.2013.03.003
Fisher, T.R., Carlson, P.R., Barber, R.T., 1982. Sediment nutrient regeneration in three North Carolina estuaries. Estuar. Coast. Shelf Sci. 14, 101–116. https://doi.org/10.1016/S0302-3524(82)80069-8
FitzJohn, R., 2019. odin: Ode Generation and Integration.
Gameiro, C., Zwolinski, J., Brotas, V., 2011. Light control on phytoplankton production in a shallow and turbid estuarine system. Hydrobiologia 669, 249–263. https://doi.org/10.1007/s10750-011-0695-3
Ganju, N.K., Brush, M.J., Rashleigh, B., Aretxabaleta, A.L., del Barrio, P., Grear, J.S., Harris, L.A., Lake, S.J., McCardell, G., O'Donnell, J., Ralston, D.K., Signell, R.P., Testa, J.M., Vaudrey, J.M.P., 2016. Progress and Challenges in Coupled Hydrodynamic-Ecological Estuarine Modeling. Estuaries and Coasts 39, 311–332. https://doi.org/10.1007/s12237-015-0011-y
Geider, R., MacIntyre, H., Kana, T., 1997. Dynamic model of phytoplankton growth and acclimation:responses of the balanced growth rate and the chlorophyll a:carbon ratio to light, nutrient-limitation and temperature. Mar. Ecol. Prog. Ser. 148, 187–200. https://doi.org/10.3354/meps148187
Gelman, A., Carlin, J.B., Stern, H.S., Dunson, D.B., Vehtari, A., Rubin, D.B., 2013. Bayesian Data Analysis, 3d ed. CRC Press.
Gelman, A., Hill, J., 2007. Data analysis using regression and multilevel/hierarchical models, Data Analysis Using Regression and Multilevel/Hierarchical Models. Cambridge University Press, New York.
Gowen, R., Tett, P., Jones, K., 1992. Predicting marine eutrophication: the yield of chlorophyll from nitrogen in Scottish coastal waters. Mar. Ecol. Prog. Ser. 85, 153–161. https://doi.org/10.3354/meps085153
Greening, H., Janicki, A., 2006. Toward Reversal of Eutrophic Conditions in a Subtropical Estuary: Water Quality and Seagrass Response to Nitrogen Loading Reductions in Tampa Bay, Florida, USA. Environ. Manage. 38, 163–178. https://doi.org/10.1007/s00267-005-0079-4
Grover, J.P., 1989. Phosphorus-dependent growth kinetics of 11 species of freshwater algae. Limnol. Oceanogr. 34, 341–348. https://doi.org/10.4319/lo.1989.34.2.0341

Haario, H., Saksman, E., Tamminen, J., 2001. An Adaptive Metropolis Algorithm. Bernoulli 7, 223. https://doi.org/10.2307/3318737

Hall, N.S., Paerl, H.W., Peierls, B.L., Whipple, A.C., Rossignol, K.L., 2013. Effects of climatic variability on phytoplankton community structure and bloom development in the eutrophic, microtidal, New River Estuary, North Carolina, USA. Estuar. Coast. Shelf Sci. 117, 70–82. https://doi.org/10.1016/j.ecss.2012.10.004

Han, Y., Aziz, T.N., Del Giudice, D., Hall, N.S., Obenour, D.R., 2021. Exploring nutrient and light limitation of algal production in a shallow turbid reservoir. Environ. Pollut. 269, 116210. https://doi.org/10.1016/j.envpol.2020.116210

Hansen, J.I., Henriksen, K., Blackburn, T.H., 1981. Seasonal distribution of nitrifying bacteria and rates of nitrification in coastal marine sediments. Microb. Ecol. 7, 297–304. https://doi.org/10.1007/BF02341424

Heisler, J., Glibert, P.M., Burkholder, J.M., Anderson, D.M., Cochlan, W., Dennison, W.C., Dortch, Q., Gobler, C.J., Heil, C.A., Humphries, E., Lewitus, A., Magnien, R., Marshall, H.G., Sellner, K., Stockwell, D.A., Stoecker, D.K., Suddleson, M., 2008. Eutrophication and harmful algal blooms: A scientific consensus. Harmful Algae 8, 3–13. https://doi.org/10.1016/j.hal.2008.08.006

Hirsch, R.M., De Cicco, L.A., 2015. User Guide to Exploration and Graphics for River Trends (EGRET) and dataRetrieval: R Packages for Hydrologic Data, Techniques and Methods book 4. https://doi.org/http://dx.doi.org/10.3133/tm4A10

Howarth, R.W., Marino, R., 2006. Nitrogen as the limiting nutrient for eutrophication in coastal marine ecosystems: Evolving views over three decades. Limnol. Oceanogr. 51, 364–376. https://doi.org/10.4319/lo.2006.51.1_part_2.0364

Jakobsen, H.H., Markager, S., 2016. Carbon-to-chlorophyll ratio for phytoplankton in temperate coastal waters: Seasonal patterns and relationship to nutrients. Limnol. Oceanogr. 61, 1853–1868. https://doi.org/10.1002/lno.10338

Katin, A., Del Giudice, D., Obenour, D.R., 2019. Modeling biophysical controls on hypoxia in a shallow estuary using a Bayesian mechanistic approach. Environ. Model. Softw. 120, 104491. https://doi.org/10.1016/j.envsoft.2019.07.016

Kelly, P.T., Renwick, W.H., Knoll, L., Vanni, M.J., 2019. Stream Nitrogen and Phosphorus Loads Are Differentially Affected by Storm Events and the Difference May Be Exacerbated by Conservation Tillage. Environ. Sci. Technol. 53, 5613–5621. https://doi.org/10.1021/acs.est.8b05152

Khalil, K., Laverman, A.M., Raimonet, M., Rabouille, C., 2018. Importance of nitrate reduction in benthic carbon mineralization in two eutrophic estuaries: Modeling, observations and laboratory experiments. Mar. Chem. 199, 24–36. https://doi.org/10.1016/j.marchem.2018.01.004

Kimmel, D.G., McGlaughon, B.D., Leonard, J., Paerl, H.W., Taylor, J.C., Cira, E.K., Wetz, M.S., 2015. Mesozooplankton abundance in relation to the chlorophyll maximum in the Neuse River Estuary, North Carolina, USA: Implications for trophic dynamics. Estuar. Coast. Shelf Sci. 157, 59–68. https://doi.org/10.1016/j.ecss.2015.02.014

Kruk, C., Huszar, V.L.M., Peeters, E.T.H.M., Bonilla, S., Costa, L., Lurling, M., Reynolds, C.S., Scheffer, M., 2010. A morphological classification capturing functional variation in phytoplankton. Freshw. Biol. 55, 614–627. https://doi.org/10.1111/j.1365-2427.2009.02298.x

Kruschke, J., 2015. Doing Bayesian data analysis: A tutorial with R, JAGS, and Stan. Academic

Press.
Lebo, M.E., Paerl, H.W., Peierls, B.L., 2012. Evaluation of Progress in Achieving TMDL Mandated Nitrogen Reductions in the Neuse River Basin, North Carolina. Environ. Manage. 49, 253–266. https://doi.org/10.1007/s00267-011-9774-5
Li, W.K.W., Lewis, M.R., Harrison, W.G., 2010. Multiscalarity of the Nutrient–Chlorophyll Relationship in Coastal Phytoplankton. Estuaries and Coasts 33, 440–447. https://doi.org/10.1007/s12237-008-9119-7
Li, Y., Liu, Y., Zhao, L., Hastings, A., Guo, H., 2015. Exploring change of internal nutrients cycling in a shallow lake: A dynamic nutrient driven phytoplankton model. Ecol. Modell. 313, 137–148. https://doi.org/10.1016/j.ecolmodel.2015.06.025
Liu, Q., Chai, F., Dugdale, R., Chao, Y., Xue, H., Rao, S., Wilkerson, F., Farrara, J., Zhang, H., Wang, Z., Zhang, Y., 2018. San Francisco Bay nutrients and plankton dynamics as simulated by a coupled hydrodynamic-ecosystem model. Cont. Shelf Res. 161, 29–48. https://doi.org/10.1016/j.csr.2018.03.008
Liu, Q.Q., Gao, Y., Xu, X.F., 2012. An Ecological Dynamics Model of Algae Growth in Taihu Lake and the Analysis of its Influencing Factors. Adv. Mater. Res. 518–523, 4961–4966. https://doi.org/10.4028/www.scientific.net/AMR.518-523.4961
Lucas, L. V, Thompson, J.K., Brown, L.R., 2009. Why are diverse relationships observed between phytoplankton biomass and transport time? Limnol. Oceanogr. 54, 381–390. https://doi.org/10.4319/lo.2009.54.1.0381
Lung, W.-S., Paerl, H.W., 1988. Modeling blue-green algal blooms in the Lower Neuse River. Water Res. 22, 895–905. https://doi.org/10.1016/0043-1354(88)90027-9
Mallin, M.A., McIver, M.R., Wells, H.A., Parsons, D.C., Johnson, V.L., 2005. Reversal of eutrophication following sewage treatment upgrades in the New River Estuary, North Carolina. Estuaries 28, 750–760. https://doi.org/10.1007/BF02732912
Malone, T.C., Conley, D.J., Fisher, T.R., Glibert, P.M., Harding, L.W., Sellner, K.G., 1996. Scales of Nutrient-Limited Phytoplankton Productivity in Chesapeake Bay. Estuaries 19, 371. https://doi.org/10.2307/1352457
Malve, O., Laine, M., Haario, H., Kirkkala, T., Sarvala, J., 2007. Bayesian modelling of algal mass occurrences—using adaptive MCMC methods with a lake water quality model. Environ. Model. Softw. 22, 966–977. https://doi.org/10.1016/j.envsoft.2006.06.016
Matson, E.A., Brinson, M.M., Cahoon, D., Davis, G.J., Dawn, C.D., Davis, G.G.J., 1983. Biogeochernistry of the Sediments of the Pamlico and Neuse River Estuaries, North Carolina, Water Resources Research Institute of the University of North Carolina. Greenville.
McSweeney, J.M., Chant, R.J., Wilkin, J.L., Sommerfield, C.K., 2017. Suspended-Sediment Impacts on Light-Limited Productivity in the Delaware Estuary. Estuaries and Coasts 40, 977–993. https://doi.org/10.1007/s12237-016-0200-3
ModMon, 2019. Neuse Estuary Modeling and Monitoring project (accessed: May 2019). http://paerllab.web.unc.edu/projects/modmon/.
Monod, J., 1949. The Growth of Bacterial Cultures. Annu. Rev. Microbiol. 3, 371–394. https://doi.org/10.1146/annurev.mi.03.100149.002103
NCCO, 2019. Meteorological data for NC. http://climate.ncsu.edu/.
NCDWQ, 2001. Total maximum daily load for total Nitrogen to the Neuse River estuary, North Carolina. Phase 2. NC Department of Environment and Natural Resources, Raleigh.
Nixon, S.W., 1995. Coastal marine eutrophication: A definition, social causes, and future concerns. Ophelia 41, 199–219. https://doi.org/10.1080/00785236.1995.10422044

Ott, W.R., 1990. A Physical Explanation of the Lognormality of Pollutant Concentrations. J. Air Waste Manage. Assoc. 40, 1378–1383. https://doi.org/10.1080/10473289.1990.10466789

Paerl, H., Mallin, M., Donahue, C., Go, M., Peierls, B.L., 1995. Nitrogen loading sources and eutrophication of the Neuse River Estuary, North Carolina: direct and indirect roles of atmospheric deposition.

Paerl, H.W., Crosswell, J.R., Van Dam, B., Hall, N.S., Rossignol, K.L., Osburn, C.L., Hounshell, A.G., Sloup, R.S., Harding, L.W., 2018a. Two decades of tropical cyclone impacts on North Carolina's estuarine carbon, nutrient and phytoplankton dynamics: implications for biogeochemical cycling and water quality in a stormier world. Biogeochemistry 141, 307–332. https://doi.org/10.1007/s10533-018-0438-x

Paerl, H.W., Hall, N.S., Peierls, B.L., Rossignol, K.L., Joyner, A.R., 2014. Hydrologic Variability and Its Control of Phytoplankton Community Structure and Function in Two Shallow, Coastal, Lagoonal Ecosystems: The Neuse and New River Estuaries, North Carolina, USA. Estuaries and Coasts 37, 31–45. https://doi.org/10.1007/s12237-013-9686-0

Paerl, H.W., Otten, T.G., Kudela, R., 2018b. Mitigating the Expansion of Harmful Algal Blooms Across the Freshwater-to-Marine Continuum. Environ. Sci. Technol. 52, 5519–5529. https://doi.org/10.1021/acs.est.7b05950

Paerl, H.W., Pinckney, J.L., Fear, J.M., Peierls, B.L., 1998. Ecosystem responses to internal and watershed organic matter loading: consequences for hypoxia in the eutrophying Neuse River Estuary, North Carolina, USA. Mar. Ecol. Prog. Ser. 166, 17–25. https://doi.org/10.3354/meps166017

Paerl, H.W., Scott, J.T., McCarthy, M.J., Newell, S.E., Gardner, W.S., Havens, K.E., Hoffman, D.K., Wilhelm, S.W., Wurtsbaugh, W.A., 2016. It Takes Two to Tango: When and Where Dual Nutrient (N & P) Reductions Are Needed to Protect Lakes and Downstream Ecosystems. Environ. Sci. Technol. 50, 10805–10813. https://doi.org/10.1021/acs.est.6b02575

Paerl, H.W., Valdes, L.M., Joyner, A.R., Piehler, M.F., Lebo, M.E., 2004. Solving Problems Resulting from Solutions: Evolution of a Dual Nutrient Management Strategy for the Eutrophying Neuse River Estuary, North Carolina. Environ. Sci. Technol. 38, 3068–3073. https://doi.org/10.1021/es0352350

Parslow, J., Cressie, N., Campbell, E.P., Jones, E., Murray, L., 2013. Bayesian learning and predictability in a stochastic nonlinear dynamical model. Ecol. Appl. 23, 679–698. https://doi.org/10.1890/12-0312.1

Peierls, B., Paerl, H., 2010. Temperature, organic matter, and the control of bacterioplankton in the Neuse River and Pamlico Sound estuarine system. Aquat. Microb. Ecol. 55, 139–149. https://doi.org/10.3354/ame01415

Peierls, B.L., Hall, N.S., Paerl, H.W., 2012. Non-monotonic Responses of Phytoplankton Biomass Accumulation to Hydrologic Variability: A Comparison of Two Coastal Plain North Carolina Estuaries. Estuaries and Coasts 35, 1376–1392. https://doi.org/10.1007/s12237-012-9547-2

Pennock, J.R., Sharp, J.H., 1992. Temporal Alteration between Light- and Nutrient-Limitation of Phytoplankton Production in a Coastal Plain Estuary, in: Primary Productivity and Biogeochemical Cycles in the Sea. Springer US, Boston, MA, pp. 525–525. https://doi.org/10.1007/978-1-4899-0762-2_62

Piehler, M.F., Thompson, S.P., Dyble, J., Moisander, P.H., Fear, J.M., Paerl, H.W., 2002. Biologically Mediated Nitrogen Dynamics in Eutrophying Esturaries. Assessing Dentrification, N2 Fixation and Primary Productivity Responses to Proposed N Loading

Reduction in the Neuse River Estuary. Water Resources Research Institute of the University of North Carolina, Report 339.
Pinckney, J.L., Paerl, H.W., Harrington, M.B., 1999. RESPONSES OF THE PHYTOPLANKTON COMMUNITY GROWTH RATE TO NUTRIENT PULSES IN VARIABLE ESTUARINE ENVIRONMENTS. J. Phycol. 35, 1455–1463. https://doi.org/10.1046/j.1529-8817.1999.3561455.x
Pinckney, J.L., Paerl, H.W., Harrington, M.B., Howe, K.E., 1998. Annual cycles of phytoplankton community-structure and bloom dynamics in the Neuse River Estuary, North Carolina. Mar. Biol. 131, 371–381. https://doi.org/10.1007/s002270050330
Pinckney, J.L., Richardson, T.L., Millie, D.F., Paerl, H.W., 2001. Application of photopigment biomarkers for quantifying microalgal community composition and in situ growth rates. Org. Geochem. 32, 585–595. https://doi.org/https://doi.org/10.1016/S0146-6380(00)00196-0
R Core Team, 2019. R: A Language and Environment for Statistical Computing.
Rabalais, N.N., Díaz, R.J., Levin, L.A., Turner, R.E., Gilbert, D., Zhang, J., 2010. Dynamics and distribution of natural and human-caused hypoxia. Biogeosciences 7, 585–619. https://doi.org/10.5194/bg-7-585-2010
Rabalais, N.N., Turner, R.E., Díaz, R.J., Justić, D., 2009. Global change and eutrophication of coastal waters. ICES J. Mar. Sci. 66, 1528–1537. https://doi.org/10.1093/icesjms/fsp047
Rachels, K.T., Ricks, B.R., 2018. Exploring Causal Factors of Spawning Stock Mortality in a Riverine Striped Bass Population. Mar. Coast. Fish. 10, 424–434. https://doi.org/10.1002/mcf2.10038
Ramin, M., Stremilov, S., Labencki, T., Gudimov, A., Boyd, D., Arhonditsis, G.B., 2011. Integration of numerical modeling and Bayesian analysis for setting water quality criteria in Hamilton Harbour, Ontario, Canada. Environ. Model. Softw. 26, 337–353. https://doi.org/10.1016/j.envsoft.2010.08.006
Redfield, A.C., Ketchum, B.H., Richards, F.A., 1963. The influence of organisms on the composition of sea-water, The Sea. John Wiley, New York.
Reichert, P., Mieleitner, J., 2009. Analyzing input and structural uncertainty of nonlinear dynamic models with stochastic, time-dependent parameters. Water Resour. Res. 45. https://doi.org/10.1029/2009WR007814
Rigosi, A., Marcé, R., Escot, C., Rueda, F.J., 2011. A calibration strategy for dynamic succession models including several phytoplankton groups. Environ. Model. Softw. 26, 697–710. https://doi.org/10.1016/j.envsoft.2011.01.007
Rizzo, W.M., Christian, R.R., 1996. Significance of Subtidal Sediments to Heterotrophically-Mediated Oxygen and Nutrient Dynamics in a Temperate Estuary. Estuaries 19, 475. https://doi.org/10.2307/1352464
Roelke, D.L., 2007. Ecology of Harmful Algae. Eos, Trans. Am. Geophys. Union 88, 304. https://doi.org/10.1029/2007EO300006
Rudek, J., Paerl, H.W., Mallin, M.A., Bates, P.W., 1991. Seasonal and hydrological control of phytoplankton nutrient limitation in the lower Neuse River Estuary, North Carolina. Mar. Ecol. - Prog. Ser. 75, 133–142.
Selberg, C.D., Eby, L.A., Crowder, L.B., 2001. Hypoxia in the Neuse River Estuary: Responses of Blue Crabs and Crabbers. North Am. J. Fish. Manag. 21, 358–366. https://doi.org/10.1577/1548-8675(2001)021<0358:HITNRE>2.0.CO;2
Smayda, T.J., 1997. Harmful algal blooms: Their ecophysiology and general relevance to phytoplankton blooms in the sea. Limnol. Oceanogr. 42, 1137–1153.

https://doi.org/10.4319/lo.1997.42.5_part_2.1137
Soetaert, K., Petzoldt, T., Setzer, R.W., 2010. Solving Differential Equations in R : Package deSolve. J. Stat. Softw. 33, 1–25. https://doi.org/10.18637/jss.v033.i09
Sorensen, T., Vasishth, S., 2015. Bayesian linear mixed models using Stan: A tutorial for psychologists, linguists, and cognitive scientists. https://doi.org/10.20982/tqmp.12.3.p175
Spruill, T.B., Bratton, J.F., 2008. Estimation of Groundwater and Nutrient Fluxes to the Neuse River Estuary, North Carolina. Estuaries and Coasts 31, 501–520. https://doi.org/10.1007/s12237-008-9040-0
Stan Development Team, 2016. RStan: the R interface to Stan (accessed: May 2016). http://mc-stan.org/.
Steele, J.H., 1965. Notes on Some Theoretical Problems in Production Ecology. Mem. dell'Istituto Ital. di Idrobiol. 18, 383.
Stone, M., 1974. Cross-Validatory Choice and Assessment of Statistical Predictions. J. R. Stat. Soc. 36, 111–147.
Stow, C.A., Roessler, C., Borsuk, M.E., Bowen, J.D., Reckhow, K.H., 2003. Comparison of Estuarine Water Quality Models for Total Maximum Daily Load Development in Neuse River Estuary. J. Water Resour. Plan. Manag. 129, 307–314. https://doi.org/10.1061/(ASCE)0733-9496(2003)129:4(307)
Strickling, H.L., Obenour, D.R., 2018. Leveraging Spatial and Temporal Variability to Probabilistically Characterize Nutrient Sources and Export Rates in a Developing Watershed. Water Resour. Res. 54, 5143–5162. https://doi.org/10.1029/2017WR022220
Taylor, D.I., Oviatt, C.A., Borkman, D.G., 2011. Non-linear Responses of a Coastal Aquatic Ecosystem to Large Decreases in Nutrient and Organic Loadings. Estuaries and Coasts 34, 745–757. https://doi.org/10.1007/s12237-010-9312-3
USGS, 2019. USGS Water Data for the Nation (accessed: May 2019). https://waterdata.usgs.gov/nwis.
Vähätalo, A. V., Zepp, R.G., 2005. Photochemical Mineralization of Dissolved Organic Nitrogen to Ammonium in the Baltic Sea. Environ. Sci. Technol. 39, 6985–6992. https://doi.org/10.1021/es050142z
Wang, J., Zhang, Z., Johnson, B., 2019. Low flows and downstream decline in phytoplankton contribute to impaired water quality in the lower Minnesota River. Water Res. 161, 262–273. https://doi.org/10.1016/j.watres.2019.05.090
Wetz, M., Paerl, H., Taylor, J., Leonard, J., 2011. Environmental controls upon picophytoplankton growth and biomass in a eutrophic estuary. Aquat. Microb. Ecol. 63, 133–143. https://doi.org/10.3354/ame01488
Whitall, D., Hendrickson, B., Paerl, H., 2003. Importance of atmospherically deposited nitrogen to the annual nitrogen budget of the Neuse River estuary, North Carolina. Environ. Int. 29, 393–399. https://doi.org/10.1016/S0160-4120(02)00175-7
Wool, T.A., Davie, S.R., Rodriguez, H.N., 2003. Development of Three-Dimensional Hydrodynamic and Water Quality Models to Support Total Maximum Daily Load Decision Process for the Neuse River Estuary, North Carolina. J. Water Resour. Plan. Manag. 129, 295–306. https://doi.org/10.1061/(ASCE)0733-9496(2003)129:4(295)
Yang, L., Peng, S., Sun, J., Zhao, X., Li, X., 2016. A case study of an enhanced eutrophication model with stoichiometric zooplankton growth sub-model calibrated by Bayesian method. Environ. Sci. Pollut. Res. 23, 8398–8409. https://doi.org/10.1007/s11356-016-6064-z